Interpretation of spectral electroluminescence images of photovoltaic modules using modelling

JL Crozier[1], **EE van Dyk and FJ Vorster**

Nelson Mandela Metropolitan University, Port Elizabeth, South Africa

E-mail: s207094248@nmmu.ac.za

Abstract. Electroluminescence (EL) is a useful solar cell and module characterisation technique as it is fast, non-destructive and sensitive to the effects of shunt and series resistance and recombination parameters. A solar cell in normal operation receives an optical input in the form of the incoming light and outputs an electrical current. Conversely, a LED receives an electrical input resulting in an optical output. EL occurs when a solar cell is forward biased receiving an electrical input and outputs an emission spectrum. The emission spectra from indirect band gap materials like silicon are in the infrared region of light while the direct band gap semiconductor materials used in LEDs emit light in the visible region. The intensity of the luminescence emitted is related to the applied voltage and the quantum efficiency of the cell material. The spectrum of the emitted luminescence can be related to the recombination properties of the cell such as surface recombination velocity and minority carrier diffusion length or lifetime. For EL imaging, a silicon CCD camera is commonly used because it has very good spatial resolution, however, this sensor is only sensitive to wavelength in the range of 300-1200 nm. There is an overlap in wavelengths from about 900 to 1100 nm allowing the EL to be detected. The spectrum of the detected EL is thus dependant on the sensitivity of the camera, the transmission of the filters and the emitted photon flux. In this study the emitted spectrum is modelled and the effects of recombination properties of the cell on the emitted spectrum are examined. The integration of short-pass filters into the experimental setup is theoretically modelled and discussed.

1. Introduction

1.1. Introduction

A solar cell and a light emitting diode (LED) can be represented as a device with electrical and optical terminals as shown in figure 1. A solar cell receives an optical input in the form of the incoming light and outputs an electrical current. Conversely a LED receives an electrical input resulting in an optical output. EL occurs in a solar cell when it is forward biased, receiving an electrical input and outputs an emission spectrum. The emission spectrum from silicon is in the infrared region of the electromagnetic spectrum[1].

A solar cell can be visualised as a spatially extended device where light is emitted at different points on the surface, each with their own local quantum efficiency and local junction voltage.

---

[1] To whom any correspondence should be addressed.

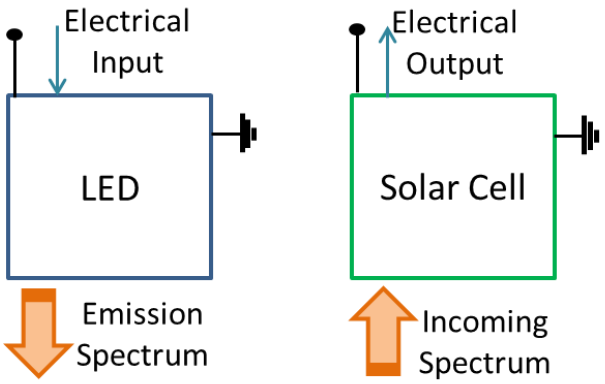

Figure 1: Solar cell represented as a device with optical and electrical terminals[2].

A detailed balance theory relating the carrier collections properties of a solar cell to the spectral EL emission is rigorously proven by U. Rau (2007)[3].

The intensity of the emitted EL at a point (x) on the cell is dependent on the reflectance ($r_f[E_\gamma]$)of photons within the material, the local internal quantum efficiency ($Q_i[E_\gamma]$) and the local junction voltages (U). These three factors relate to classical loss mechanisms namely, optical, recombination and resistive losses[2]. If the local junction voltage is assumed to be constant across the cell, the relationship between the optical and recombination properties and the spectrum of the emitted EL of the cell can be investigated.

1.2. Charge carrier distribution

When a forward bias is applied to a solar cell, minority carriers are injected at the p-n junction. Electrons are injected at the p-side of the p-n junction and holes at the n-side. Since the n-layer (emitter) is very thin, the amount of radiative recombination occurring is negligible[4]. Thus the distribution of electrons in the p-side of the p-n junction is discussed in this section.

The minority carrier concentration, n_e, at the junction (z=0) is given in equation (1) and is dependent on the intrinsic carrier concentration, n_i, the doping concentration of the base, N_A, applied junction voltage, U, and the thermal voltage, k_BT/e [1]:

$$n_e(0) = \frac{n_i^2}{N_A}\exp\left(\frac{eU}{k_BT}\right). \quad (1)$$

The carrier concentration at the rear surface, *ne(d),* is related to the surface recombination velocity (S), the carrier diffusivity (D_e) and the charge carrier diffusion current density (j_e), as follows:

$$j_e(d) = -D_e\frac{dn_e}{dx}(d) = Sn_e(d) \quad (2)$$

The carrier diffusion length is related to carrier diffusivity and carrier lifetime (τ_e):

$$L_e = \sqrt{D_e\,\tau_e} \quad (3)$$

These boundary conditions allow the minority carrier distribution, *n(z),* to be determined as a function of applied voltage, diffusion length and rear surface recombination velocity. Electrons are injected at the junction (z= *0*) where the concentration is given by equation (1) and dependent on intrinsic carrier concentration, the doping concentration of the base, the applied junction voltage, U, and the thermal voltage, k_BT/e. An increase in the applied junction voltage will increase the carrier concentration which results in increase radiative recombination which leads to an increase in EL intensity. In this study the modelling of the EL spectrum is discussed with respect to recombination such as diffusion length and surface recombination velocity.

1.3. Photon Emission under forward bias

The rate of spontaneous photoemission by a semiconductor can be determined using a generalised form of Planck's law of radiation of non-black bodies[4].

The rate of spontaneous photoemission of photons of energy, E_γ, in a certain volume element is given by:

$$r_{sp}(E_\gamma) = \alpha(E_\gamma)\frac{{E_\gamma}^2}{\pi^2\hbar^3c^2}\frac{1}{exp\left(\frac{E_\gamma-\Delta\eta}{k_BT}\right)-1} \quad . \tag{4}$$

Where $\alpha(E_\gamma)$ is the energy-dependant absorption coefficient, $\hbar$ is the reduced Planck's constant, c, is the speed of light, $\Delta\eta$ is the local separation of quasi-Fermi Energies, k_B is Boltzmann's constant and T is temperature in Kelvin.

The quasi-Fermi levels of n- or p- type Silicon can be related to the doping concentration (N_A), the intrinsic equilibrium charge carrier concentration (n_i) and the carrier distribution ($n(z)$).

Low- injection conditions are assumed with recombination occurring through band-band transitions [5]. The dependence of the recombination parameters on the carrier concentration is ignored in order to get a numerically solvable equation. Further assumptions are made that carrier diffusion does not occur laterally in the cell, only parallel to the depth. These assumptions allow the rate of spontaneous photoemission to be approximated using:

$$r_{sp}(E_\gamma, z) \approx \alpha(E_\gamma)\frac{{E_\gamma}^2}{\pi^2\hbar^3c^2}exp\left(-\frac{E_\gamma}{k_BT}\right)\frac{N_A\frac{n(z)}{D}}{n_i^2} \quad . \tag{5}$$

Equation (5) predicts the local spectral distribution of spontaneously emitted photons within the sample.

1.4. Emitted Photon Detection

The rate at which of photons of an certain energy interval, $I(E_\gamma)$, are emitted from the surface of the cell sample can be obtained by integrating equation 4 across the thickness of the cell and is given by equation (6).

$$I(E_\gamma) = \left[1 - R_f(E_\gamma)\right]\int_0^d (r_{sp}(z, E_\gamma)\{exp[-\alpha(E_\gamma)z] + R_r(E_\gamma)\exp[-\alpha(E_\gamma)(2d - z)]\})dz \tag{6}$$

The reflectance terms take into account a single reflection from the front surface (R_f) and at the rear surface (R_r). The inclusion of the absorption coefficient, $\alpha(E_\gamma)$, in the equation takes into account the reabsorption of photons in their optical path to the surface of the cell. The generation of electron-hole pairs due to reabsorption of these spontaneously emitted photons is ignored as non-radiative recombination is assumed to be the dominant form of recombination [1]. Equation (6) only considers photons emitted normal to the cell surface.

For EL imaging, a silicon CCD camera is commonly used because it has very good spatial resolution, however, it is only sensitive to wavelengths in the range of 300-1200 nm[6]. There is an overlap in wavelengths from about 900 to 1100 nm allowing the EL to be detected. InGaAs cameras can also be used for EL imaging and have a wider spectral detection range. However, they lack the spatial resolution of silicon and since they are more sensitive to longer wavelengths, they are more susceptible to light trapping within the sample which results in smearing of the image[1].

The spectrum of the detected EL is thus dependant on the sensitivity of the camera (Φ_{camera}), the transmission of filters (T_{filter}) used and the emitted photon flux[1] as shown:

$$I_{detect}(E_\gamma) = T_{filter}(E_\gamma)\Phi_{camera}(E_\gamma)\, I(E_\gamma) \quad . \tag{7}$$

2. Experimental Setup

2.1. Modeling

The results are modelled using a Mathematica routine. The parameters used are given in table 1. These parameters are used unless otherwise specified and are literature values or from Kirchartz et.al.[7].

Table 1. The parameters used for modelling the EL spectrum of Silicon.

Parameter	**Symbol**	**Value used**
Intrinsic carrier concentration	n_i	9.69×10^{15} m^{-3} at 300 K
Doping concentration of the base	N_A	10^{22} m^{-3} at 300 K
Temperature	T	300 K
Local Junction Voltage	U	0.05 mV
Surface Recombination Velocity	S	10 m/s
Diffusion length	Le	100 µm
Electron diffusivity	De	27×10^{-4} $m.s^{-1}$
Thickness of p-layer	d	250 µm
Speed of light	c	2.998×10^{8} $m.s^{-1}$
Reduced Planck's constant	ħ	6.58×10^{-4} eV.s
Boltzmann's constant	k_B	8.617×10^{-5} $eV.K^{-1}$

3. Results

3.1. Modeling of excess charge carrier distribution

The effects of recombination properties on the charge carrier distribution is modelled using equations 1 and 2 and the parameters of table 1. Figure 2 shows the excess carrier concentration of electrons in the p-side of a solar cell with a thickness of 250 µm. The distribution of minority carriers across the depth of the cell is determined by the diffusion length of the carriers and by increasing the diffusion length, the distribution of carriers across the cell increases. The surface recombination velocity, S, is the rate at which carriers recombine at the surface of the material and is set at 10 $m.s^{-1}$. The faster recombination occurs at the surface, the lower the carrier concentration at the surface (z=250 µm).

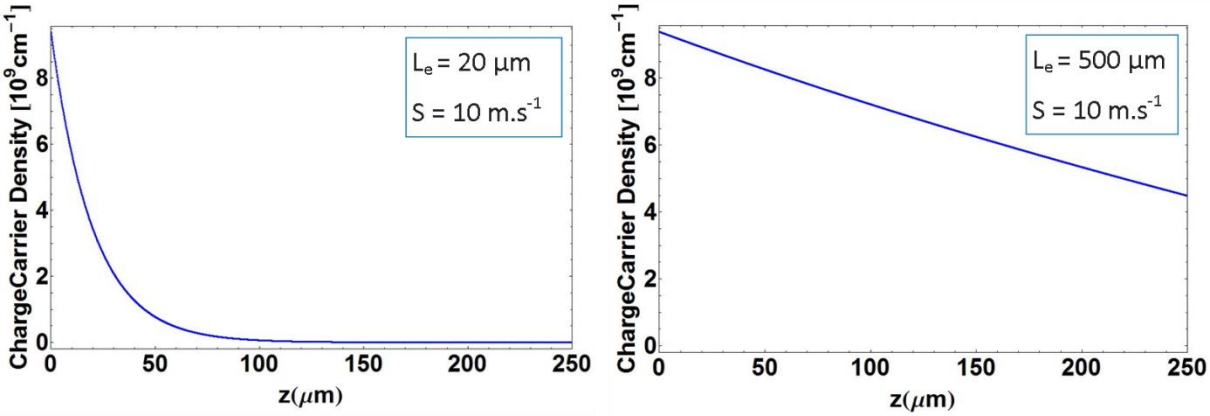

Figure 2: Excess charge carrier distribution across the depth of the cell modelled with diffusion lengths equal to 20µm and 500µm.

3.2. Modeling of detected EL

The EL intensity, which is the rate of photons emitted from a local surface element is simulated and plotted against wavelength in figure 3. Varying the diffusion length of the carriers has a more significant effect on the short wavelength region of the spectrum. High energy (short wavelength) photons are

more likely to be re-absorbed as silicon has a higher absorption coefficient in the low wavelength region. A short diffusion length means the carriers recombine deeper in the cell close to the p-n junction and the photons are more likely to be reabsorbed before they can be emitted at the surface. A longer diffusion length means carriers are able to recombine further away from the junction closer to the surface and thus the number of emitted photons of all energies is greater. This effect is especially noticeable in the short wavelength, high EL photon energy region.

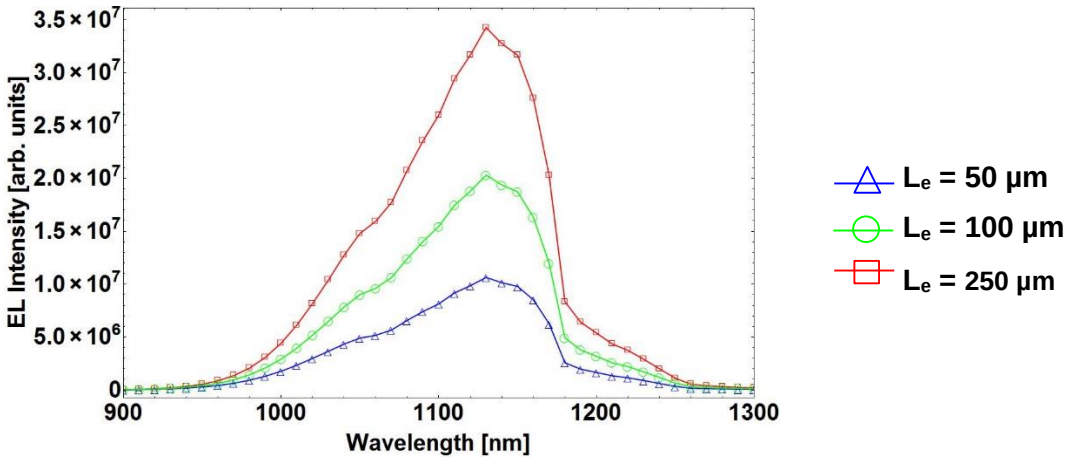

Figure. 3: The EL spectrum modeled at different diffusion lengths.

3.3. Detecting EL using a CCD camera

Figure 4 shows the overlap of the modeled EL spectrum and the CCD sensitivity[8], and short-pass filters with cut-offs at 900 nm and 1000 nm. The overlap between the CCD camera and the EL spectrum is only at short wavelengths and thus only a small percentage of the total EL can actually be detected. The incorporation of short-pass filters was suggested by Wurfel et al[1], in order to isolate only photons emitted from EL in the short wavelength region. These photons are generated near the surface as high energy photons generated deeper would be reabsorbed. The use of filters limits the spectrum of the detected EL and thus the image can be spectrally defined.

Figure 5 shows the CCD camera's quantum efficiency, the modelled EL and the detected EL. The EL and quantum efficiency are normalised. The detected EL is in the wavelength range of between 950-1150 nm which includes only a small portion of the total emitted EL in the region where the camera has low quantum efficiency.

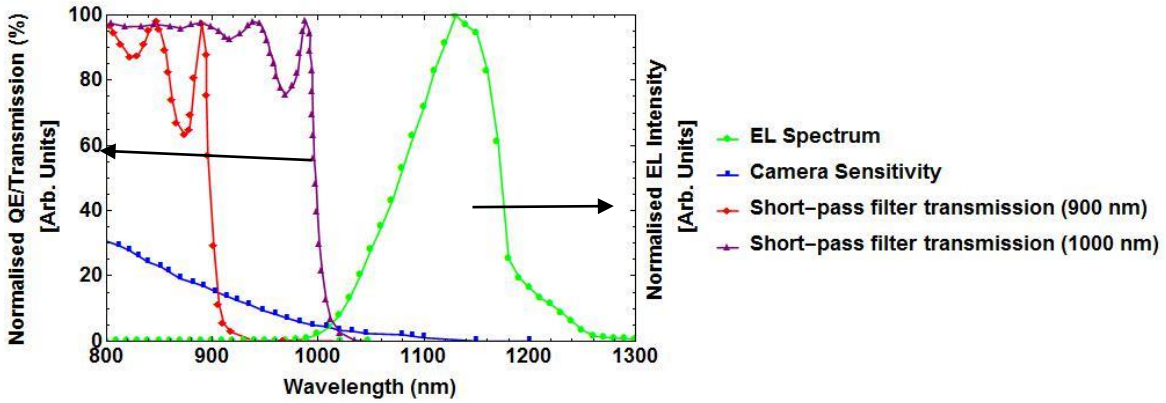

Figure 4: The EL spectrum overlaid with the CCD camera sensitivity and the transmission of the short-pass filters.

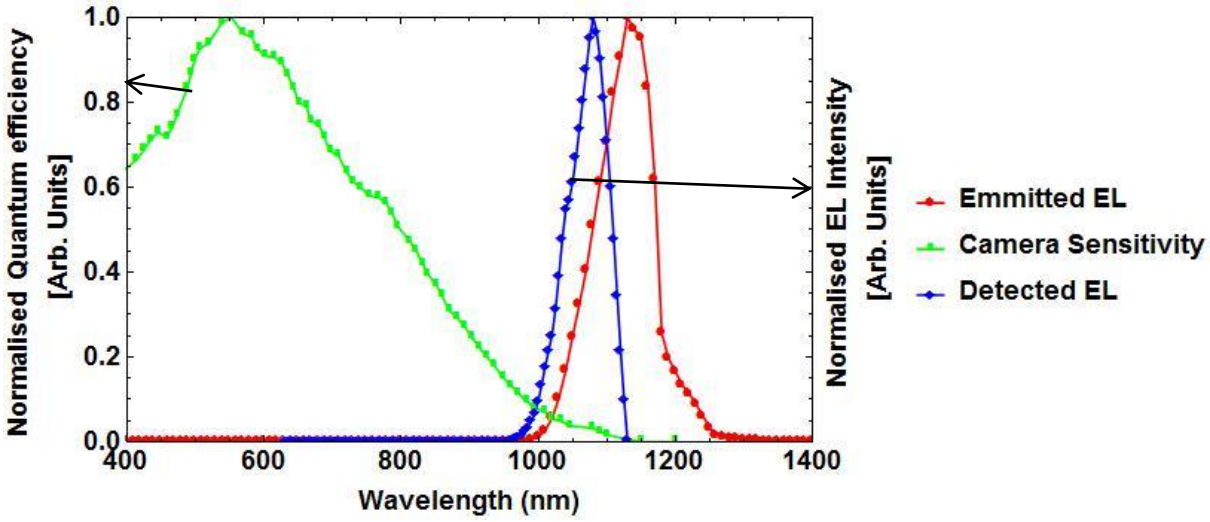

Figure 5: The EL spectrum of silicon modelled with parameters set in table 11 compared with the silicon CCD camera sensitivity. The normalised detected EL peak is also plotted.

4. Discussion and Conclusion

A solar cell can be visualised as a spatially extended device where light is emitted at different points on the surface, each with their own local quantum efficiency and local junction voltage.

A thorough understanding of the spectrum of emitted during EL is important. Modelling the effects of different recombination properties and filter integration allows for a better idea of the EL process. While the EL imaging with a silicon CCD camera is not able to measure the EL spectrum the use of filters allows some assumptions of the detected wavelength range to be made. The modeled EL spectrum illustrated that the minority carrier diffusion length has an effect on the EL intensity in the short wavelength region. As this region is within the detection sensitivity of the camera, the modeling of the effects of diffusion is important for interpreting the EL images. Future work includes integration of filters into experimental set-up and correlation between experimental and simulated results.

Lateral filter inhomogeneity in the short-pass filters can cause a significant variation in the transmission of the filter. This needs to be addressed in future experimental work, possibly by rotating the filter and averaging the images.

5. References

[1] Würfel P, Trupke T, Puzzer T, Schäffer E, Warta W, Glunz SW 2007 *J Appl Phys* **101** 123110.
[2] Kirchartz T, Helbig A, Reetz W, Reuter M, Werner JH, Rau U 2009 *Prog Photov* **17** 394-402.
[3] Rau U 2007 *Phys Rev B: Condens Matter* **76**.
[4] Giesecke JA, Kasemann M, Warta W 2009 *J Appl Phys* **106** 014907.
[5] Rißland S, Breitenstein O 2013 *Sol Energy Mater Sol Cells* **111** 112-4.
[6] Fuyuki T, Kitiyanan A 2008 *Appl Phys A*.**96** 189-96.
[7] Kirchartz T, Helbig A, Rau U 2008 *Sol Energy Mater Sol Cells* **92** 1621-7.
[8] Sensovation. SensoCam Scientific Cameras. 2012 [cited 2014 10 July]; Available from: http://www.sensovation.com/bausteine.net/f/10339/web_SensoCamA4single.pdf?fd=2.